Microcapsules

Deutsche Ausgabe: DOI: 10.1002/ange.201605905
Internationale Ausgabe: DOI: 10.1002/anie.201605905

Multilayer Microcapsules for FRET Analysis and Two-Photon-Activated Photodynamic Therapy

Yang Yang, Huiling Liu, Mingjuan Han, Bingbing Sun, and Junbai Li**

Abstract: *Microcapsules obtained by layer-by-layer assembly provide a good platform for biological analysis owing to their component diversity, multiple binding sites, and controllable wall thickness. Herein, different assembly species were obtained from two-photon dyes and traditional photosensitizers, and further assembled into microcapsules. Fluorescence resonance energy transfer (FRET) was shown to occur between the two-photon dyes and photosensitizers. Confocal laser scanning microscopy (CLSM) with one- and two-photon lasers, fluorescence lifetime imaging microscopy (FLIM), and time-resolved fluorescence spectroscopy were used to analyze the FRET effects in the microcapsules. The FRET efficiency could easily be controlled through changing the assembly sequence. Furthermore, the capsules are phototoxic upon one- or two-photon excitation. These materials are thus expected to be applicable in two-photon-activated photodynamic therapy for deep-tissue treatment.*

Förster (fluorescence) resonance energy transfer (FRET) is a mechanism for describing the energy transfer between two light-sensitive molecules (usually fluorophores). In this process, an excited-state donor fluorophore transfers energy to a proximal ground-state acceptor fluorophore through non-radiative dipole–dipole coupling.[1,2] The FRET efficiency strongly depends on several factors, such as the extent of the spectral overlap, the quantum yield of the fluorophores, and, most importantly, the distance between donor and acceptor (D/A, proximity of 1–10 nm).[3,4] In general, the FRET rate is inversely proportional to the sixth power of this distance, making FRET extremely sensitive to small changes in the distance between donor and acceptor. Therefore, FRET has been used to measure the distance between D/A molecules and to detect molecular interactions in a number of systems, and has applications in biology and chemistry.[1,4–6] Beyond that, in recent years, the application of FRET has been extended to cancer research, for example, in photodynamic therapy (PDT).[7–10]

PDT is a form of phototherapy that uses photosensitizers (PSs); these are selectively exposed to light whereupon they become toxic to the targeted malignant and other diseased cells. However, the PSs widely used in clinical PDT absorb in the visible region below $\lambda = 700$ nm, where light penetration into the skin is only a few millimeters.[11] Some emerging approaches offer new perspectives for improving the PDT treatment depth through coupling PSs with two-photon dyes or particles in the confined space of nanosystems.[9,10,12–17] PSs can be excited indirectly with two-photon-absorbing (TPA) dyes through the FRET mechanism. Two-photon-activated PDT (TPA-PDT) offers several advantages over conventional one-photon PDT, such as reduced photoinduced damage, enhanced imaging resolution of turbid samples, and, most importantly, an extended PDT window (i.e., 700–1000 nm) for deep-tissue treatment. However, such TPA-PDT systems must be carefully designed, and it is difficult to control the FRET process and its efficiency.

The layer-by-layer (LbL) assembly technique offers a simple and versatile way to build functional films on different substrates by cyclic adsorption of a polycation and a polyanion.[18–23] This makes LbL multilayers containing different dyes ideally suited for studying FRET processes between different dyes. The groups of Jonas and Reynolds have systematically studied the FRET processes between multilayer films containing donor and acceptor dyes.[24,25] Herein, we fabricated LbL multilayer polyelectrolyte microcapsules. A suitable TPA dye and a traditional PS were selected and conjugated with different polyelectrolyte layers. Furthermore, the PS could be indirectly activated by TPA dyes in the multilayer system through the one- or two-photon-induced FRET mechanism (see the Supporting Information, Figure S1). The FRET efficiency could also be easily controlled through changing the assembly method or adjusting the assembly sequences. This approach provides possibilities for improving the two-photon absorption cross-sections of traditional photosensitizers using the molecular assembly method. Therefore, this system could be applied in TPA-PDT to improve the treatment depth. Although LbL microcapsules have been developed for decades, to the best of our knowledge, this is the first report of using LbL microcapsules to study FRET mechanisms and for TPA-PDT applications. Compared with other approaches towards TPA-PDT,[9,10,12,13] this system should be simpler and easier to control.

The LbL microcapsules were typically fabricated by cyclic adsorption of a polycation (poly(allylamine), PAH) and

[*] Dr. Y. Yang, H. L. Liu, Prof. Dr. J. B. Li
CAS Center for Excellence in Nanoscience
CAS Key Laboratory for Biomedical Effects of Nanomaterials and Nanosafety, National Center for Nanoscience and Technology
Zhong Guan Cun, Bei Yi Tiao 11, Beijing, 100190 (China)
B. B. Sun, Prof. Dr. J. B. Li
Key Lab of Colloid, Interface and Chemical Thermodynamics
Institute of Chemistry, Chinese Academy of Sciences
Zhong Guan Cun, Bei Yi Jie 2, Beijing, 100190 (China)
E-mail: jbli@iccas.ac.cn
H. L. Liu, Prof. Dr. M. J. Han
College of Chemistry and Molecular Engineering
Nanjing Tech University
Puzhu South Road 30, Nanjing, 210009 (China)
E-mail: hmjcaj@njtech.edu.cn

Supporting information for this article can be found under: http://dx.doi.org/10.1002/anie.201605905.

a polyanion (poly(sodium-*para*-styrenesulfonate), PSS) on the surface of a $MnCO_3$ microsphere template (Figure S1). Before adsorption, the PAH was labeled with a TPA dye (fluorescein isothiocyanate, FITC) and a PS dye (Rose Bengal, RB), in a coupling reaction to yield the functional components FITC-PAH and RB-PAH, respectively. In some reports, FITC and RB acted as standard TPA dyes and photosensitive drugs in PDT.[10,26] The spectral overlap between the maximum emission of FITC and the maximum absorption of RB was investigated in our previous work. This spectral overlap enables their use as a FRET pair.[12] In this work, the corresponding spectra of FITC-PAH and RB-PAH were characterized, which also featured an overlapping region (over 30%, Figure S2), enabling FRET. Subsequently, as the first system in this work, positively charged FITC-PAH and RB-PAH were first mixed and then alternatingly adsorbed with negatively charged PSS until ten bilayers had been assembled on the surface of the $MnCO_3$ particles. The surface zeta potential was determined after the deposition of every polymer layer on the particle surface (Figure S3), which confirmed the LbL process during material preparation. Furthermore, $((FITC\text{-}PAH + RB\text{-}PAH)/PSS)_{10}$ microcapsules (denoted as FR capsules) were obtained after removing the $MnCO_3$ cores. The morphological characteristics of the FR capsules are shown in Figure S4. The average thickness of a single PAH/PSS bilayer was calculated as approximately 4 nm by atomic-force microscopy (AFM; Figure S4c). This thickness is consistent with a similar, previously reported structure.[27–29] In general, the distance between a donor dye and an acceptor dye has to be less than 10 nm for efficient FRET.[6] Therefore, we believe that the layered space in the capsule wall is very suitable for FRET pairs. The sample was also examined by confocal laser scanning microscopy (CLSM). As shown in Figure S4d–f, green fluorescence represented the FITC-conjugated PAH, while red fluorescence represented the RB-conjugated PAH. The superimposed image confirmed that FITC and RB co-existed in the microcapsule walls. The green fluorescence was weaker than the red fluorescence owing to intra-capsule FRET effects, which will be discussed below.

The donor (D) can be quenched by the acceptor (A); accordingly, the donor fluorescence lifetime will be reduced and the acceptor fluorescence lifetime will be increased if a FRET process takes place between the D/A dyes.[30] On the other hand, the fluorescence intensity of a donor dye will increase if we forcefully quench the acceptor dye.[31] Based on these properties, the FRET effect was validated using several methods for the FR-Capsules system. First, acceptor dyes (RB) in a local region of the FR-Capsules were selected to be bleached with a high-intensity 559 nm laser, while ones beyond this region were not. We found that the FR-Capsules did not show the green fluorescence of the donor dyes (FITC) before bleaching the RB, which confirmed that FITC transferred energy to the RB (Figure 1a). On the contrary, the regions in which RB was bleached showed strong green fluorescence because there was no energy acceptor (Figure 1b). On the other hand, after the RB in the microcapsules had been bleached, the selected time-lapse images in Figure S5 showed that the fluorescence intensity of RB gradually

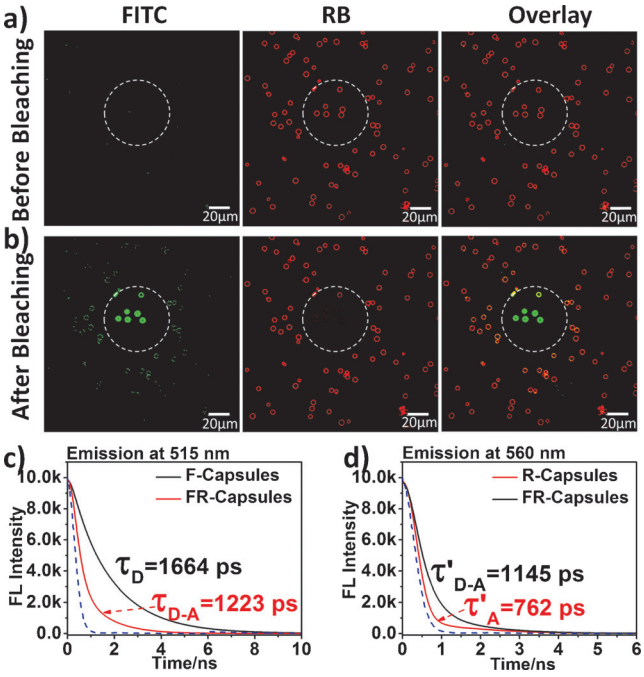

Figure 1. CLSM images of FR-Capsules a) before and b) after bleaching of a selected area (white circles) for 15 s. Fluorescence decay curves of c) F-Capsules and FR-Capsules detected at 515 nm (λ_{max} of FITC) and d) R-Capsules and FR-Capsules detected at 560 nm (λ_{max} of RB) at $\lambda_{ex} = 455$ nm. The blue dashed line represents the instrument response.

decreased, whereas the fluorescence intensity of FITC increased as time progressed. Time-resolved fluorescence measurements were also used to analyze the FRET process of the microcapsules. For comparison, PAH labeled with a single dye (FITC or RB) was used for assembly with PSS for preparing single FITC-labeled capsules (F-Capsules) and single RB-labeled capsules (R-Capsules), respectively. For the FR-Capsules, the average lifetime of the fluorescence decay at 515 nm was 1223 ps (τ_{D-A}), which was shorter than that of the F-Capsules ($\tau_D = 1664$ ps; Figure 1c). Meanwhile, the average lifetime of the FR-Capsules ($\tau'_{D-A} = 1145$ ps) at 560 nm was longer than that of the R-Capsules ($\tau'_A = 762$ ps; Figure 1d). These results also suggested that effective FRET occurred between the FITC-PAH and RB-PAH layers in the microcapsule walls. The FRET efficiency was calculated as $E_{FRET}(\%) = \left(1 - \frac{\tau'_A}{\tau'_{D-A}}\right) \times 100\% = 33.4\%$.

Furthermore, a CLSM equipped with a two-photon laser (TP-CLSM) was used to validate the two-photon absorption and two-photon FRET of the samples. As shown in Figure 2, the FR-Capsules also showed strong green (495–540 nm) and red fluorescence (575–630 nm) after excitation with the two-photon laser (920 nm), confirming that the capsules underwent two-photon absorption. In detail, F-Capsules were mixed with the same amount of FR-Capsules and studied using TP-CLSM. Obviously, there were two types of capsules with different intensities of green fluorescence (Figure 2a, FITC channel) even though the FITC content in the F- and FR-Capsules was exactly the same. We believe that the low-intensity green microcapsules are the FR-Capsules while the

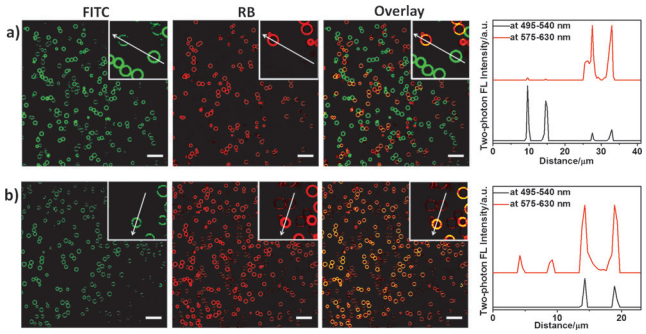

Figure 2. TP-CLSM images of mixed microcapsules a) composed of the same amount of FR-Capsules and F-Capsules, and b) composed of the same amount of FR-Capsules and R-Capsules. The excitation wavelength was 920 nm, and fluorescence was collected at 495–540 nm (FITC channel) and 575–630 nm (RB channel). The corresponding fluorescence intensity profiles along the indicated lines for two selected capsules are shown on the right. Scale bars: 20 μm. The FITC content of the FR-Capsules and F-Capsules, and also the RB content of the FR-Capsules and R-Capsules, was kept the same by using UV monitoring.

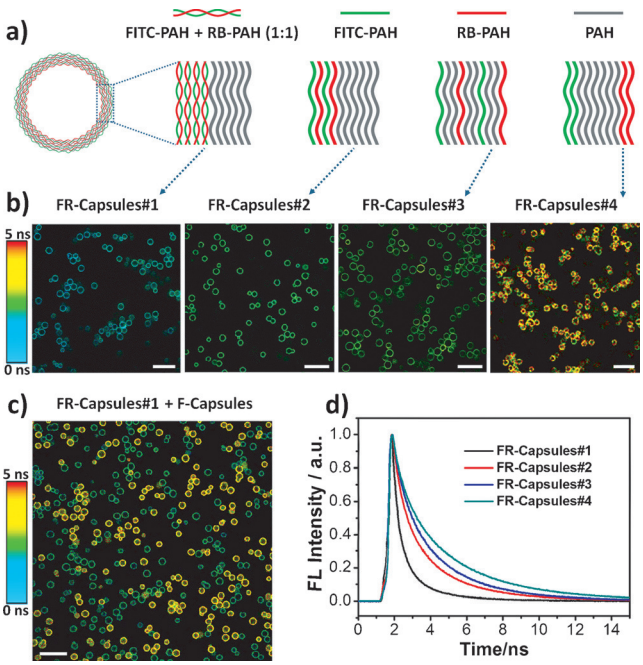

Figure 3. a) Illustration of FR-Capsules with different assembly sequences of FITC-PAH, RB-PAH, and PAH. A negatively charged PSS layer is present between two adjacent positively charged PAH layers, which are not shown in the diagram. The FITC and RB contents of these capsule systems were kept the same by using UV monitoring. b) FLIM images with $\lambda_{ex} = 485$ nm ($\lambda_{em} = 499$–539 nm) for FR-Capsules#1 to FR-Capsules#4. c) Mixed microcapsules composed of the same amount of FR-Capsules#1 and F-Capsules. d) The corresponding lifetime decay curves of different microcapsule systems. Scale bars: 20 μm.

high-intensity green microcapsules represented the F-Capsules. It is easy to understand that FITC was quenched by RB in the FR-Capsules through the two-photon-activated FRET mechanism. In the overlay image in Figure 2a, two types of microcapsules could be distinguished: The orange capsules represent FR-Capsules, and the green capsules represent F-Capsules. These capsules could also be separated clearly in the corresponding fluorescence intensity profiles. Similarly, the R-Capsules were mixed with the same amount of FR-capsules and analyzed with the same method. As shown in Figure 2b, low-intensity red microcapsules represent the R-Capsules while the high-intensity red microcapsules represent the FR-Capsules (RB channel). This is due to the fact that FITC units in FR-Capsules transfer their energy to RB, which increases the fluorescence intensity of RB.

Förster theory states that the FRET efficiency varies with the sixth power of the distance between donor and acceptor. For the FR-Capsules, the distance between FITC and RB could be controlled through adjusting the assembly method and the number of layers. Therefore, four capsule systems were prepared with different assembly sequences for a fluorescence lifetime imaging microscopy (FLIM) analysis. As shown in Figure 3a, the assembly processes of these capsules were entirely the same, except for inserting different numbers of PAH layers with no fluorophore among the FITC-PAH and RB-PAH layers for adjusting the distance between FITC and RB. The amount of FITC/RB was kept the same in every capsule system by monitoring their characteristic UV absorption. In fact, unlike the fluorescence intensity, the fluorescence lifetime is not dependent on the donor concentration, illumination intensity, and moderate photobleaching. Therefore, FLIM is considered as the most rigorous method for measuring FRET. In this work, the fluorescence lifetime of the donor FITC in different capsule systems was imaged as shown in Figure 3b. Obviously, the fluorescence lifetime of FITC increased with the distance between the FITC-PAH and RB-PAH layers. In these systems, the fluorescence lifetime of FITC was shortest in the FR-Capsules#1, which implied a minimum distance between FITC and RB. The FRET efficiency of FR-Capsules#1 was approximately 51% as analyzed with FLIM software. Meanwhile, the fluorescence lifetime of FITC in FR-Capsules#4 was longer than that of other capsules because FITC and RB were separated by more PAH layers with no fluorophore. The FR-Capsules#4 presented the lowest FRET efficiency (ca. 6%). This was also confirmed by the lifetime decay curves in Figure 3d. Furthermore, an equimolar mixture of FR-Capsules#1 and F-Capsules was analyzed by FLIM (Figure 3c). The blue circles with a short lifetime represent FR-Capsules#1, in which FITC was quenched by RB. The yellow circles with a long lifetime represent F-Capsules, which do not contain an energy acceptor for quenching FITC.

The generation of cytotoxic singlet oxygen from FR-Capsules was detected indirectly using a reactive oxygen indicator (ABDA). The characteristic absorption peak of ABDA will decrease in intensity with an increase in the singlet oxygen concentration in solution.[32,33] After addition of ABDA into the FR-Capsules suspension and irradiation with 480 nm light (λ_{max} of FITC), a rapid decrease in the ABDA absorbance intensity was observed with increasing exposure time (Figure 4a). For the FR-Capsules, the relative absorbance of ABDA at 400 nm decreased to 8.2% after 80 min of irradiation, whereas it was 31.0% for the same amount of pure RB (Figure 4b). Pure RB led to a slower

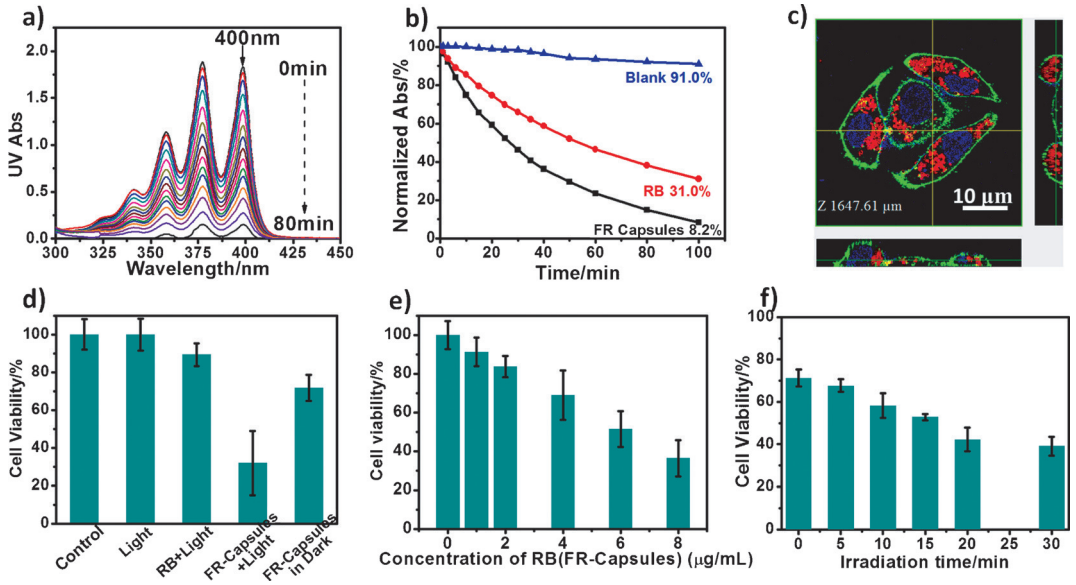

Figure 4. a) Absorption spectra of ABDA in the presence of FR-Capsules under irradiation at 480 nm over different periods of time. b) Normalized absorbance change of ABDA at 400 nm against irradiation time in the presence of FR-Capsules (black line) and the same amount of RB (red line). c) 3D reconstruction CLSM image of HeLa cells (cytomembrane green, nucleus blue) co-cultured with FR-Capsules (red) for 3 h; the orthogonal section images at the bottom and on the right were recorded along the yellow lines. d) Viability of HeLa cells under various conditions. (The concentrations of both pure RB and the capsules containing RB in the cell culture media were 10 $\mu g\,mL^{-1}$.) e) Viability of HeLa cells co-cultured with various concentrations of FR-Capsules under irradiation with a 480 nm laser for 10 min. (The concentration of the FR-Capsules is expressed in terms of the RB component of the capsules in cell culture media, as below.) f) Viability of HeLa cells co-cultured with FR-Capsules and irradiated for different periods of time; the concentration of the RB component in the capsule suspension in the cell culture media was 4 $\mu g\,mL^{-1}$.

decrease in the absorbance intensity of ABDA because the irradiation wavelength of 480 nm is not the maximum excitation wavelength for RB. These results confirmed that FR-Capsules produce singlet oxygen with high efficiency when exposed to 480 nm light. They also indirectly corroborated the occurrence of FRET between FITC-PAH and RB-PAH in the FR-Capsules.

FR-Capsules were co-cultured with HeLa cells to study their cytotoxicity under different conditions. For improving the endocytosis efficiency, smaller FR-Capsules (S-FR-Capsules, ca. 2 µm; their morphology is shown in Figure S6) were prepared according to the same method, except that a smaller $MnCO_3$ template was used. As shown in Figure S7 and Figure 4c, the assembled capsules were easily internalized into cancer cells when they were co-cultured for 5 h in the dark. Incidentally, compared with the strong green fluorescence from cell membrane dyes (Alex 488), the capsules did not show green fluorescence upon excitation with a 488 nm laser owing to the intra-capsule FRET effects. The strong red fluorescence of the FR-Capsules inside the cytoplasm implied that capsules had been captured by cells. The cytotoxicity of internalized FR-Capsules to HeLa cells was evaluated using an MTT assay before and after exposure to a Xe lamp with a 480 nm filter. As shown in Figure 4d, the cell viability decreased sharply in the presence of FR-Capsules after exposure to light. However, the same amount of pure RB did not cause obvious cytotoxicity under the same conditions. This is due to several reasons: 1) For the soluble RB, it was difficult to cross cell membranes to reach the interior of cells; 2) the lifetime of singlet oxygen was very short, and it was difficult for the produced singlet oxygen from the RB solution to directly act on the organelle; and 3) 480 nm is not the maximum absorption wavelength for RB. Conversely, the FR-Capsules could bind and directly carry RB into the interior of cells. After exposure to 480 nm light irradiation, the FITC units transferred their energy to RB moieties within the same capsule, which produced singlet oxygen that directly acted on the organelle. Therefore, the FR-Capsules are cytotoxic under irradiation. Furthermore, the light cytotoxicity of FR-Capsules was investigated at different concentrations and for different irradiation times. It was found that the light cytotoxicity of the FR-Capsules increased with the sample concentration (Figure 4e) and the irradiation time (Figure 4f). In the range that is shown there, a nearly linear relationship between the cytotoxicity and the sample concentration, as well as irradiation time, was found.

The two-photon-induced cytotoxicity of the FR-Capsules was further studied by TP-CLSM. HeLa cells were cultured with FR-Capsules for 4 h and then irradiated by a 920 nm two-photon laser for 10 min, followed by continuous culturing for another 16 h. A specific dye, propidium iodide (PI), was added to the cultured media to identify dead cells.[34] The in situ CLSM images of PI cellular staining, together with differential interference contrast (DIC) transmission light images, illustrate the TP-PDT effect. As shown in Figure 5c, the dispersed green/red fluorescence spots in the FITC and RB channel represent the internalized FR-Capsules in the first 4 h. However, after irradiation with the two-photon laser, many of the cells were stained with red PI (Figure 5d), which confirmed that cellular apoptosis had been induced and the

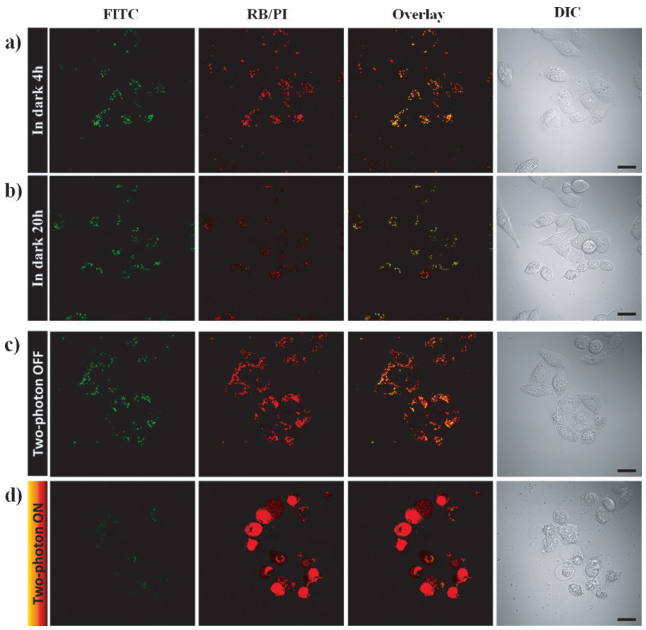

Figure 5. In situ observation of HeLa cells by CLSM: Cells co-cultured with FR-Caspules#1 for 4 h (a) and 20 h (b) in the dark; HeLa cells co-cultured with FR-Caspules#1 for 4 h (c), and then irradiated using a 920 nm two-photon laser for 10 min followed by continuous culturing for another 16 h (d). Scale bars: 20 μm.

high two-photon toxicity of the materials. As a control experiment, HeLa cells were co-cultured with FR-Capsules for 4 h and 20 h in the dark, and analyzed by in situ CLSM (Figure 5a,b). During this period, the cells were not stained by PI, which confirmed the low cytotoxicity of the materials in the dark. In another control experiment, HeLa cells were cultured without the capsules and irradiated with the two-photon laser with the same parameters as for CLSM observation in situ. Low two-photon toxicity was observed (Figure S8). These results show that the FR-Capsules could induce two-photon toxicity in cancer cells. The two-photon toxicity induced by the reactive oxygen species is due to excited RB. The RB was excited indirectly by the two-photon dye (FITC) through intra-capsule FRET mechanisms.

In conclusion, we have successfully assembled LbL microcapsules that were used for one- or two-photon-induced PDT. The assembled species were composed of a two-photon dye and a photosensitizer-labeled polyelectrolyte, FITC-PAH and RB-PAH. FITC-PAH can be excited with a one- or two-photon laser and can transfer its energy to RB-PAH through an intra-capsule FRET mechanism. Therefore, RB can be excited indirectly with a one- or two-photon laser. The FRET efficiency between FITC-PAH and RB-PAH in the capsules could be adjusted by changing the assembly sequence. The microcapsules have low cytotoxicity in the dark and high cytotoxicity after irradiation with either a one- or two-photon laser. These results highlight possibilities for improving the two-photon absorption cross-sections of traditional photosensitizers by using the molecular assembly method. Furthermore, this technique provides a possible solution for applying traditional photosensitizers in two-photon-induced PDT.

Acknowledgements

This work was financially supported by the National Nature Science Foundation of China (21273055, 21433010, 21320102004, 21321063, and 21003074), the National Basic Research Program of China (2013CB932800), the National Key Foundation for Exploring Scientific Instrument (2013YQ16055108), the Natural Science Foundation of Jiangsu Province (BK20131407), and the open project of the CAS Key Laboratory for Biomedical Effects of Nanomaterials and Nanosafety (NSKF201608). We thank Dr. Luru Dai for helpful discussions and Dr. Hongyan Zhang for FLIM analysis.

Keywords: dyes · FRET · microcapsules · photodynamic therapy · photosensitizers

How to cite: *Angew. Chem. Int. Ed.* **2016**, *55*, 13538–13543
Angew. Chem. **2016**, *128*, 13736–13741

[1] K. E. Sapsford, L. Berti, I. L. Medintz, *Minerva Biotechnol.* **2004**, *16*, 253–279.
[2] J. R. Lakowicz, *Principles of Fluorescence Spectroscopy*, 2nd Ed., Kluwer Academic Press/Plenum Publishers, New York, **1999**.
[3] L. Stryer, *Annu. Rev. Biochem.* **1978**, *47*, 819–846.
[4] E. A. Jares-Erijman, T. M. Jovin, *Nat. Biotechnol.* **2003**, *21*, 1387–1395.
[5] A. Miyawaki, A. Sawano, T. Kogure, *Nat. Cell Biol.* **2003**, S1–S7.
[6] K. E. Sapsford, L. Berti, I. L. Medintz, *Angew. Chem. Int. Ed.* **2006**, *45*, 4562–4589; *Angew. Chem.* **2006**, *118*, 4676–4704.
[7] E. Yaghini, A. M. Seifalian, A. J. MacRobert, *Nanomedicine* **2009**, *4*, 353–363.
[8] J. M. Tsay, M. Trzoss, L. Shi, X. Kong, M. Selke, M. E. Jung, S. Weiss, *J. Am. Chem. Soc.* **2007**, *129*, 6865–6871.
[9] S. Kim, T. Y. Ohulchanskyy, H. E. Pudavar, R. K. Pandey, P. N. Prasad, *J. Am. Chem. Soc.* **2007**, *129*, 2669–2675.
[10] S.-H. Cheng, C.-C. Hsieh, N.-T. Chen, C.-H. Chu, C.-M. Huang, P.-T. Chou, F.-G. Tseng, C.-S. Yang, C.-Y. Mou, L.-W. Lo, *Nano Today* **2011**, *6*, 552–563.
[11] A. Ormond, H. Freeman, *Materials* **2013**, *6*, 817.
[12] H. Liu, Y. Yang, A. Wang, M. Han, W. Cui, J. Li, *Adv. Funct. Mater.* **2016**, *26*, 2561–2570.
[13] J. Valanciunaite, A. S. Klymchenko, A. Skripka, L. Richert, S. Steponkiene, G. Streckyte, Y. Mely, R. Rotomskis, *RSC Adv.* **2014**, *4*, 52270–52278.
[14] X. Zhuang, X. Ma, X. Xue, Q. Jiang, L. Song, L. Dai, C. Zhang, S. Jin, K. Yang, B. Ding, P. C. Wang, X.-J. Liang, *ACS Nano* **2016**, *10*, 3486–3495.
[15] J. Schmitt, V. Heitz, A. Sour, F. Bolze, H. Ftouni, J.-F. Nicoud, L. Flamigni, B. Ventura, *Angew. Chem. Int. Ed.* **2015**, *54*, 169–173; *Angew. Chem.* **2015**, *127*, 171–175.
[16] X. Shen, S. Li, L. Li, S. Q. Yao, Q.-H. Xu, *Chem. Eur. J.* **2015**, *21*, 2214–2221.
[17] A. Chaix, K. El Cheikh, E. Bouffard, M. Maynadier, D. Aggad, V. Stojanovic, N. Knezevic, M. Garcia, P. Maillard, A. Morere, M. Gary-Bobo, L. Raehm, S. Richeter, J.-O. Durand, F. Cunin, *J. Mater. Chem. B* **2016**, *4*, 3639–3642.
[18] G. Decher, *Science* **1997**, *277*, 1232–1237.
[19] P. Bertrand, A. Jonas, A. Laschewsky, R. Legras, *Macromol. Rapid Commun.* **2000**, *21*, 319–348.
[20] K. Ariga, Y. Yamauchi, G. Rydzek, Q. Ji, Y. Yonamine, K. C. W. Wu, J. P. Hill, *Chem. Lett.* **2014**, *43*, 36–68.
[21] T. Lee, S. H. Min, M. Gu, Y. K. Jung, W. Lee, J. U. Lee, D. G. Seong, B.-S. Kim, *Chem. Mater.* **2015**, *27*, 3785–3796.

[22] K. Ariga, K. Minami, M. Ebara, J. Nakanishi, *Polym. J.* **2016**, *48*, 371 – 389.
[23] W. Cui, J. Li, G. Decher, *Adv. Mater.* **2016**, *28*, 1302 – 1311.
[24] S. Peralta, J. L. Habib-Jiwan, A. M. Jonas, *ChemPhysChem* **2009**, *10*, 137 – 143.
[25] Q. Bricaud, R. M. Fabre, R. N. Brookins, K. S. Schanze, J. R. Reynolds, *Langmuir* **2011**, *27*, 5021 – 5028.
[26] Ł. Moczek, M. Nowakowska, *Biomacromolecules* **2007**, *8*, 433 – 438.
[27] E. Donath, G. B. Sukhorukov, F. Caruso, S. A. Davis, H. Möhwald, *Angew. Chem. Int. Ed.* **1998**, *37*, 2201 – 2205; *Angew. Chem.* **1998**, *110*, 2323 – 2327.
[28] K. S. Mayya, D. I. Gittins, A. M. Dibaj, F. Caruso, *Nano Lett.* **2001**, *1*, 727 – 730.
[29] S. Ai, G. Lu, Q. He, J. Li, *J. Am. Chem. Soc.* **2003**, *125*, 11140 – 11141.
[30] A. K. Kenworthy, *Methods* **2001**, *24*, 289 – 296.
[31] J. B. Dictenberg, W. Zimmerman, C. A. Sparks, A. Young, C. Vidair, Y. Zheng, W. Carrington, F. S. Fay, S. J. Doxsey, *J. Cell Biol.* **1998**, *141*, 163 – 174.
[32] I. Roy, T. Y. Ohulchanskyy, H. E. Pudavar, E. J. Bergey, A. R. Oseroff, J. Morgan, T. J. Dougherty, P. N. Prasad, *J. Am. Chem. Soc.* **2003**, *125*, 7860 – 7865.
[33] X.-L. Wang, Y. Zeng, Y.-Z. Zheng, J.-F. Chen, X. Tao, L.-X. Wang, Y. Teng, *Chem. Eur. J.* **2011**, *17*, 11223 – 11229.
[34] A. Moore, C. J. Donahue, K. D. Bauer, J. P. Mather in *Methods in Cell Biology*, *Vol. 57* (Eds.: P. M. Jennie, B. David), Academic Press, New York, **1998**, pp. 265 – 278.

Received: June 18, 2016
Published online: August 16, 2016

